Journal of
Nanomedicine & Nanotechnology

Sanyal et al. J Nanomedic Nanotechnol 2011, 2:7
DOI: 10.4172/2157-7439.1000126

Research Article Open Access

Thermo-Responsive Core-Shell Composite Nanoparticles Synthesized via One-Step Pickering Emulsion Polymerization for Controlled Drug Delivery

Sriya Sanyal, Huang-Chiao Huang, Kaushal Rege and Lenore L. Dai*

School for Engineering of Matter, Transport and Energy, Arizona State University, Tempe, AZ 85287, USA

Abstract

Purpose: The focus of this work is to develop a unique drug delivery vehicle which can be taken up by cancer cells and can release the loaded drug.

Methods: Core-shell composite nanoparticles have been prepared by one-step Pickering emulsion polymerization with a nonionic initiator, using silica as the sole stabilizer. More importantly, the Pickering emulsion polymerization is applied to synthesize polystyrene/poly(N-isopropylacrylamide) (PNIPAAm)-silica core-shell nanoparticles with N-isopropylacrylamide incorporated into the core as a co-monomer.

Results: The composite nanoparticles are temperature sensitive and can be taken up by human prostate cancer (PC3 and PC3-PSMA) cells. An anticancer agent 17-(Allylamino)-17-demethoxygeldanamycin (17-AAG) has been loaded into the polymeric cores during formation of the nanoparticles and drug release has been successfully observed at elevated temperatures. The ability of the various nanoparticles for inducing death in human prostate cancer cells has been evaluated.

Conclusion: The work has demonstrated the temperature sensitivity, controlled drug release properties of the synthesized core-shell nanoparticles, and their effectiveness for inducing death of human prostate cancer cells.

Keywords: Pickering emulsion polymerization; Composite nanoparticles; Temperature sensitivity; Drug release; Cytotoxicity

Introduction

Nanoparticles are receiving increasing attention since they have properties that are significantly different than those of bulk materials [1,2]. The high surface-to-volume ratio of nanoparticles makes them a suitable carrier or delivery system for drugs, proteins or genes which can be either delivered locally or targeted specifically [3]. Organic-inorganic composites are vital in biological and medical applications such as in artificial bones, dental fillings, and drug delivery [4]. Among them, core-shell composite nanoparticles are a unique class of materials which are attractive for their potential applications as delivery vehicles (for drugs, dyes, cosmetics, ink etc.) [5,6]. Core-shell composite particles can be synthesized by methods of post-surface-reaction [7,8], electrostatic deposition [9], and layer-by-layer self-assembly [10-12]. Here we employ the concept of Pickering emulsions to synthesize core-shell composite particles. Pickering emulsion polymerization is superior in several aspects: (1) no sophisticated instrumentation is needed; (2) a commercialized nanoparticle powder or solution can be used without further treatment; (3) the synthesis can be completed in one-step; and (4) the produced particle dispersion is surfactant-free which makes it easier to purify and an excellent material for biological applications. Despite these advantages, efforts made to explore and utilize the Pickering approach have been scarce, although some related synthesis methods have been documented including miniemulsion polymerization [13,14], dispersion polymerization [15,16], inverse suspension polymerization [17,18], and inverse emulsion polymerization [19] stabilized by fine solid particles. It is worthwhile to note that the composite nanoparticle structure in this study is opposite to the often reported core-shell structure in which inorganic particles serve as the core and polymer serves as the shell [10,20-24]. Here the polymer serves as the core and the inorganic particles serve as the shell. Such materials provide a new class of supramolecular building blocks and can "exhibit unusual, possibly unique, properties which cannot be obtained simply by co-mixing polymer and inorganic particles" [25].

"Smart" materials that respond to environmental changes, such as temperature or pH, are attractive means for designing "intelligent" drug carrier systems. In this study, N-isopropylacrylamide (NIPAAm) is incorporated as a co-monomer in order to impart temperature sensitivity to the core-shell nanoparticles. Poly (N-isopropylacrylamide) (PNIPAAm) is a well-understood temperature sensitive gel, which undergoes volume shrinkage at a transition temperature of approximately 32°C in pure water [26]. Below this temperature which is referred to as the lower critical solution temperature (LCST), the polymer chain is hydrophilic because the hydrogen bonding between the hydrophilic groups and water molecules dominates; above the LCST, the polymer chain becomes hydrophobic due to the weakened hydrogen bonding at elevated temperatures and the interactions among hydrophobic groups [27]. To synthesize PNIPAAm chains in solutions, techniques such as free radical initiation in organic solutions, redox initiation in aqueous medium, ionic initiators, and radiation of aqueous medium are used [28]. One advantage of using PNIPAAm is that it can be engineered to possess transition temperatures slightly above physiological temperatures (e.g., at 38-39°C) [29], that can be exploited for selective and controlled delivery at the tumor site using external stimuli (e.g. laser irradiation) which is suitable for triggered *in vivo* drug delivery. Recently a "nanopump" system was reported using block copolymer poly(L-lactide-star block-N-isopropylacrylamide)

***Corresponding author:** Lenore L. Dai, School for Engineering of Matter, Transport and Energy, Arizona State University, Tempe, AZ 85287, USA, Tel: 480-965-4112; Fax: 480-727-9321; E-mail: Lenore.Dai@asu.edu

Received November 20, 2011; **Accepted** December 23, 2011; **Published** December 26, 2011

Citation: Sanyal S, Huang H, Rege K, Dai LL (2011) Thermo-Responsive Core-Shell Composite Nanoparticles Synthesized via One-Step Pickering Emulsion Polymerization for Controlled Drug Delivery. J Nanomedic Nanotechnol 2:126. doi:10.4172/2157-7439.1000126

(PLLA-sb-PNIPAAm) for controlled drug release [30]. The PNIPAAm block leads to the shrinkage of the complex micelles and pumps the drug out when the temperature is above the LCST. However, the nanoparticles constructed out of the block polymer have a tendency to aggregate together if the temperature is above the LCST [31]. This was likely due to the loss of amphiphilic property of the block copolymer above the LCST as PNIPAAm blocks transformed into their hydrophobic character. In this work, we report a different synthetic pathway and use Pickering emulsion polymerization which provides adequate stability as evidenced by zeta potential measurements. Cancer drug candidate 17-(Allylamino)-17-demethoxygeldanamycin (17-AAG), an ansamycin antibiotic, which binds and inhibits Heat Shock Protein 90 (HSP 90), is incorporated into the core during synthesis and used as a hydrophobic drug in the release experiments. Figure 1 illustrates a synthesized core-shell "smart" nanoparticle and its release of drugs upon temperature change. Cellular uptake and cytotoxicity were studied in prostate cancer cells incubated at 37°C, with composite nanoparticles encapsulating 17-AAG and their controls.

Experimental Section

Materials

IPA-ST (Nissan Chemicals) is a dispersion of 10-15 nm silica nanoparticles in 2-isopropanol at a concentration of 30-31 wt %. Nonionic azo initiator VA-086 (98%, 2,2-azobis(2-methyl-*N*-(2-hydroxyethyl)propionamide), Wako Chemicals), styrene monomer (99.9%, Fisher), N-isopropylacrylamide monomer (NIPAAm, 97%, Aldrich), and water (HPLC grade, Acro Organics) were used in the polymerization without further purification. The nonpolar dye BODIPY (493/503) (4,4-difluoro-1,3,5,7,8-pentamethyl-4-bora-3a,4a-diaza-s-indacene) was obtained from Invitrogen, Molecular Probes. The serum-free medium contains RPMI-1640 medium, 25 mM HEPE, L-Glutamine, and 1% Penicillin/streptomycin (HyClone). The serum-containing medium has 10% FBS (heat inactivated fetal bovine serum, HyClone) in addition to the serum-free medium. PC3-PSMA prostate cancer cells were generous gifts from Dr. Michael Sadelain at the Memorial Sloan Kettering Cancer Center, New York and were used as provided; PC3-PSMA cells are a sub-clone of PC3 cells retrovirally transduced to stably express the PSMA receptor [32]. PC3 cells were purchased from ATCC. The drug candidate, 17-(Allylamino)-17-demethoxygeldanamycin (17AAG) was obtained from LC Laboratories, MA. 3-(4, 5- dimethylthiazol-2-yl)-2, 5-diphenyl tetrazolium bromide (MTT) was the assay (ATCC Inc.) used in cytotoxicity experiments.

Composite nanoparticle synthesis

Water, IPA-ST, NIPAAm and styrene were agitated mechanically with an IKA Ultra Turrax T25 homogenizer at 10,800 rpm for 2 min in an ice bath to emulsify. Then, the emulsion was degassed with nitrogen and kept in nitrogen atmosphere under magnetic stirring. When the temperature was raised to 70°C, the initiator aqueous solution was added to start the polymerization which lasted for 5 hours. The dye BODIPY493/503, when used for cellular uptake experiments, was added prior to adding the initiator. A typical formulation of the thermo-responsive nanoparticle includes 0.66 g NIPAAm, 3.76 g styrene, 32 mL water, 4.1 g IPA-ST silica nanoparticle dispersion, 0.037 g initiator VA-086, and 1 μg BODIPY 493/503. For the release experiments, 17AAG was added to the emulsion before the polymerization took place, prior to adding the initiator at a concentration of 600 g/ml. The drug, 17AAG, remained stable, as determined from comparing its Fourier transform infrared spectroscopy (FTIR) spectra before and after heating for 5 hours at 70°C. Before characterization, release and uptake experiments, the synthesized nanoparticles were washed twice by centrifuging-redispersing cycles using an Eppendorf 5810R centrifuge.

Characterization methods

Particle size distribution and zeta potential of composite particles were measured using a Brookhaven 90Plus Particle Size Analyzer with the dynamic light scattering (DLS) technique. The washed composite particles were further dispersed to appropriate concentrations with water before measurements. Specimens for electron microscope were prepared by placing a droplet of polymer samples onto mica substrates and dried in air. The specimens were then sputter coated with gold and viewed by SEM-XL30 (FEI). Fourier transform infrared spectra (FTIR)

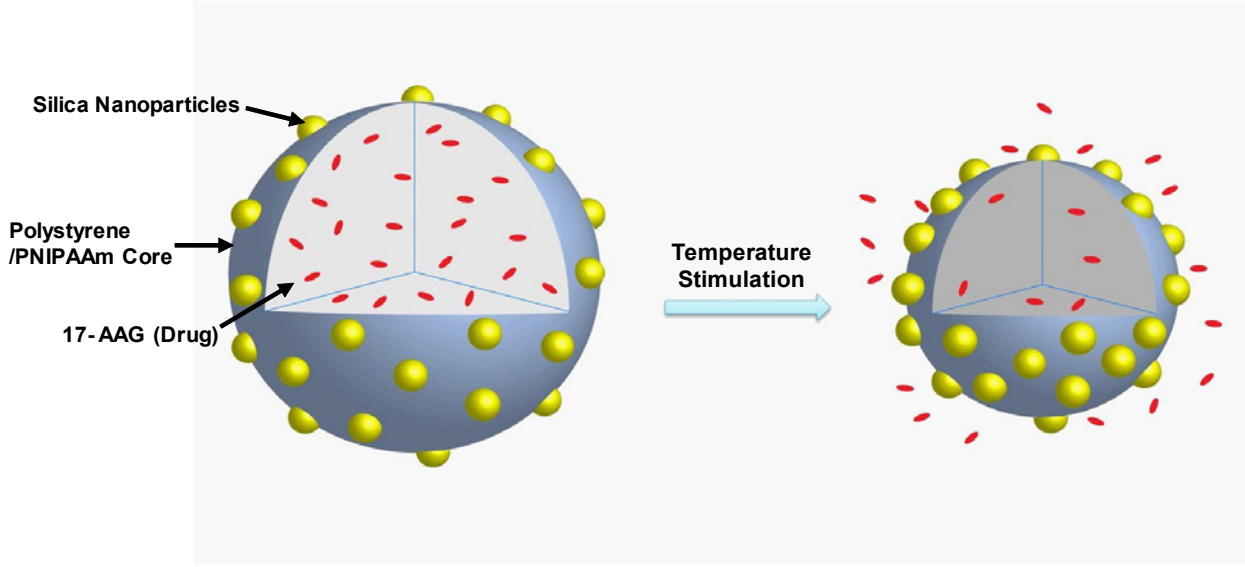

Figure 1: Schematic illustration of the polystyrene/PNIPAAm composite nanoparticles responding to temperature change and releasing encapsulated drugs.

were scanned over the range of 400-4000 cm^{-1} with potassium bromide pellet on a Bruker IFS 66V/S FTIR spectrometer. To remove the silica shell, hydrofluoric acid (HF) etching procedure described by Han and coworkers [33] was adopted.

Cellular uptake experiments

Composite core-shell nanoparticles were loaded with BODIPY 493/503 dye in the core using methods described above. Dye-loaded nanoparticles were employed in cellular uptake experiments, in concert with confocal microscopy. PC3 and PC3-PSMA prostate cancer cells were seeded in a 24-well plate at a density of 50,000 per well and incubated overnight at 37°C and 5% CO_2. Dye-loaded nanoparticles were added to cancer cells in the absence of serum for 0.5, 1.0, 1.5, and 5 h following which, the nanoparticle-containing medium was removed and cells were washed five times using 1X phosphate buffered saline (PBS). Cells were stained with the nuclear stain Hoechst 33258 (MP Biomedicals) and then mounted for analysis using a laser scanning Nikon C2 confocal microscope (Nikon Instruments Inc., Melville, NY). Images were acquired and stacked using NIS-Elements Microscope Imaging Software (Nikon Corporation) at 60× water objective with a z-step of 0.4 µm slice and with PMT scanners at 1024 × 1024 pixels.

Drug loading and release experiments

Composite core-shell nanoparticles loaded with 17AAG were used for the drug release experiments. The drug release study was done by centrifugation, after the nanoparticles were centrifuged and the supernatant was collected and tested for drug release. The amount of drug released was determined by UV analysis. Absorbance (at a wavelength of 332 nm) of a number of standard solutions of the reference substance at concentrations encompassing the sample concentrations was measured using a Biotek Microplate Reader and the calibration graph was constructed.

Cytotoxicity experiments

The cytotoxicity of nanoparticles (NPs) was determined using 3-(4, 5- dimethylthiazol-2-yl)-2, 5-diphenyl tetrazolium bromide (MTT) assay. Prostate cancer cells were cultured in medium (RPMI 1640 plus 10 % fetal bovine serum and 1% penicillin/streptomycin) under 5% CO_2 at 37°C. Cells were seeded in a 96-well plate at a cell density of 5,000 cells per well and allowed to attach overnight prior to NP treatment (0.01-1 µg/ml). At 72 h after treatment with different doses of NPs, 10 µl of MTT reagent was added to each well and incubated under 5% CO_2 at 37°C for 4 h, followed by addition of detergent. Absorbance at 570 nm was determined with microplate reader (Biotek Synergy 2). Studies were performed with at least 4 individual samples and repeated 3 times. Any interference from NPs alone (i.e. without cells) was normalized for all samples. Two-tailed Student's t-test was employed for statistical analysis.

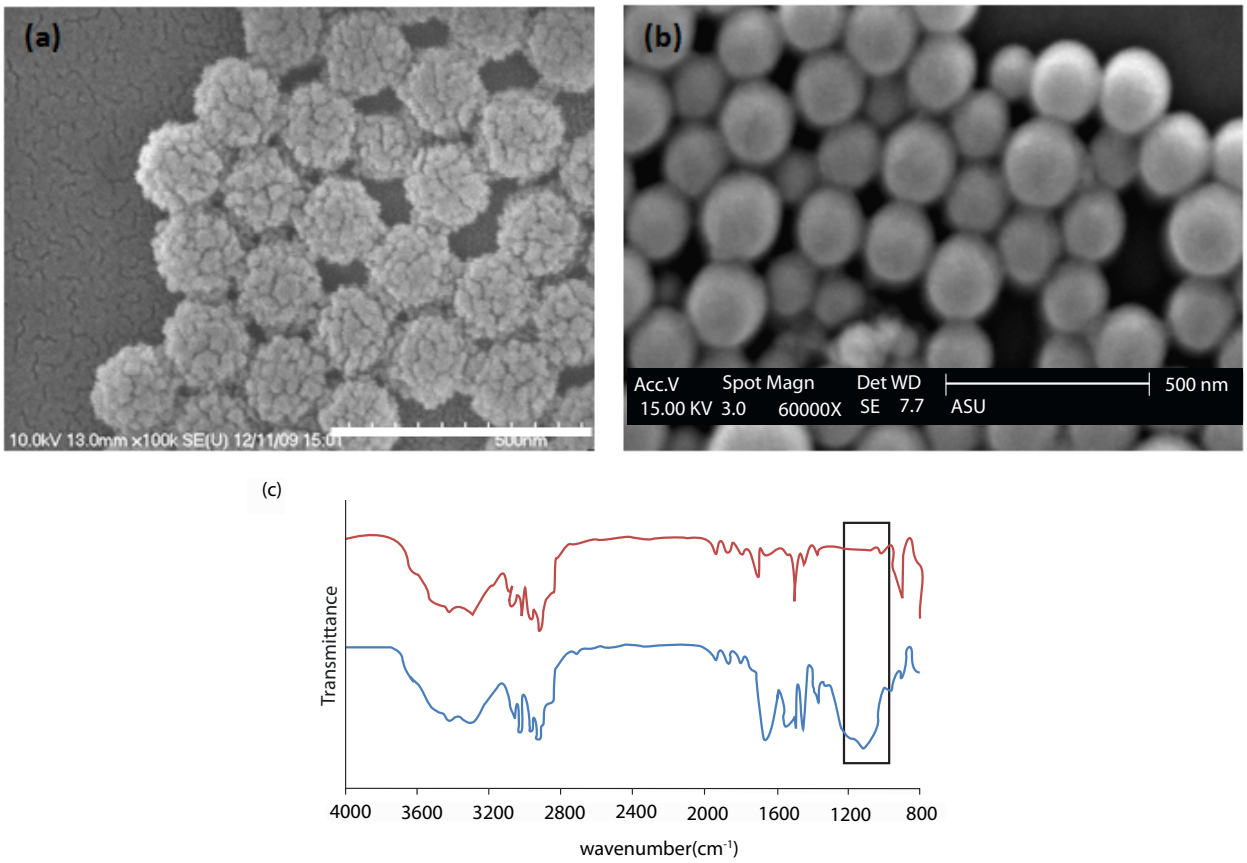

Figure 2: (a) An SEM image of the composite particles (b) SEM image taken after HF etching process (the scale bar represents 500 nm). (c) An FTIR spectrum of the composite nanoparticles where the blue line represents the composite particles and the red line is a sample of composite particles treated with HF. The box highlights the difference between the two spectra near 1104 cm^{-1} which corresponding to the asymmetrical vibration of the Si-O-Si bond.

Results and Discussion

Composite nanoparticle synthesis

Different ratios of styrene/NIPAAm were used in the formulation of the polystyrene/PNIPAAm-silica core-shell nanoparticles. It was found that when the concentration of PNIPAAm is high, the volume change of the nanoparticles is more significantly greater with change in temperature. Here we present the studies using the percentage of 15% NIPAAm. Pickering emulsion polymerization was performed using VA-086 as the initiator. In order to verify the sole stabilizing effect of silica nanoparticles, emulsifier-free emulsion polymerization using VA-086 as the initiator in the absence of silica nanoparticles was also conducted. No particle formation was observed in the product, as evidenced by SEM images. These experiments suggest that the initiator VA-086 has little effect on stabilizing in emulsion polymerization and therefore silica nanoparticles are the only source of stabilizer when present [34,35]. Figure 2(a) is a representative SEM image of the composite particles sampled at 5-hour reaction time which shows that the particles tend to be spherical. The roughness of the composite particle surfaces suggests that the composite particles are covered by silica nanoparticles; this is contrasted by the smooth surface of the hydrofluoric acid (HF)-treated particles in Figure 2(b). HF dissolves the silica layer and leaves behind the smooth polymer surface. It is also evidenced by the blue line in the FTIR spectrum in Figure 2(c) which shows that the composite particles have a characteristic strong peak at 1104 cm^{-1}, corresponding to the asymmetrical vibration of the Si-O-Si bond. Such a peak is absent in the red line in Figure 2(c) which represents the HF-treated composite particles. FTIR is a strong analytical tool which gives information about specific chemical bonds simply by interpreting the infrared absorption spectrum; here it is used to identify the presence of silica. The core-shell structure of the nanoparticles has also been confirmed by transmission electron microscope (TEM) images of polystyrene-silica nanoparticle cross-sections [34]. The measurement of zeta potential allows predictions about the storage stability of a colloidal dispersion. Particle aggregation is less likely to occur for charged particles (high zeta potential) due to electric repulsion. The mean zeta potential for the drug loaded polystyrene/PNIPAAm-silica nanoparticles was -48.1 mV. Therefore, this system has a relative good stability and dispersion quality.

Thermoresponsiveness of the composite particles

The synthesized polystyrene/PNIPAAm-silica core-shell nanoparticles are responsive to thermal stimuli. Figure 3(a) shows the dependence of average diameter of the composite particles on temperature. The average particle size at 25°C is approximately 92 nm. The size decreases sharply as the temperature reaches 32°C, around the LCST for homopolymer PNIPAAm and size change is nearly reversible upon cooling. Control experiments of polystyrene-silica nanoparticles did not show a size transition over a temperature range of 25-45°C (data not shown). The transition temperature is not shifted by the silica nanoparticle encapsulation. This is consistent with the recently reported composite microspheres with a PNIPAAm core and a silica shell which also show a volume transition starting at 32°C [17]. It is likely due to the fact that silica particles are physically adsorbed on the surfaces of PNIPAAm microspheres thus no chemical bond formation with silica occurs which might change the transition temperature. Moreover, the copolymerization with styrene has no significant effect on the transition temperature. One hypothesis is the relative phase separation of PNIPAAm and polystyrene within the core. Duracher et al. [36] studied PNIPAAm-polystyrene particles and suggest a PNIPAAm-rich shell and a polystyrene-rich core structure. Such phase separation may also occur in the core of the composite particles here although detailed morphology is unknown.

Drug release, cell-uptake and cytotoxicity

The drug candidate used in the release experiment is 17-AAG, an ansamycin antibiotic which binds to Hsp90 (Heat Shock Protein 90). Hsp90 plays a key role in regulating the physiology of cells exposed to environmental stress and in maintaining the malignant phenotype of tumor cells. Hsp90 client proteins are important in the regulation of the cell cycle, cell growth, cell survival, apoptosis, and oncogenesis. 17-AAG binds with a high affinity into the domain of adenosine triphosphate (ATP) binding pocket in Hsp90 and induces the degradation of proteins that require it for conformational maturation. Heat Shock Protein 90 (Hsp90) is of significant interest in cancer therapy because it helps in cell survival and tumor cell proliferation. The main obstacle to the delivery of 17-AAG is its poor water solubility

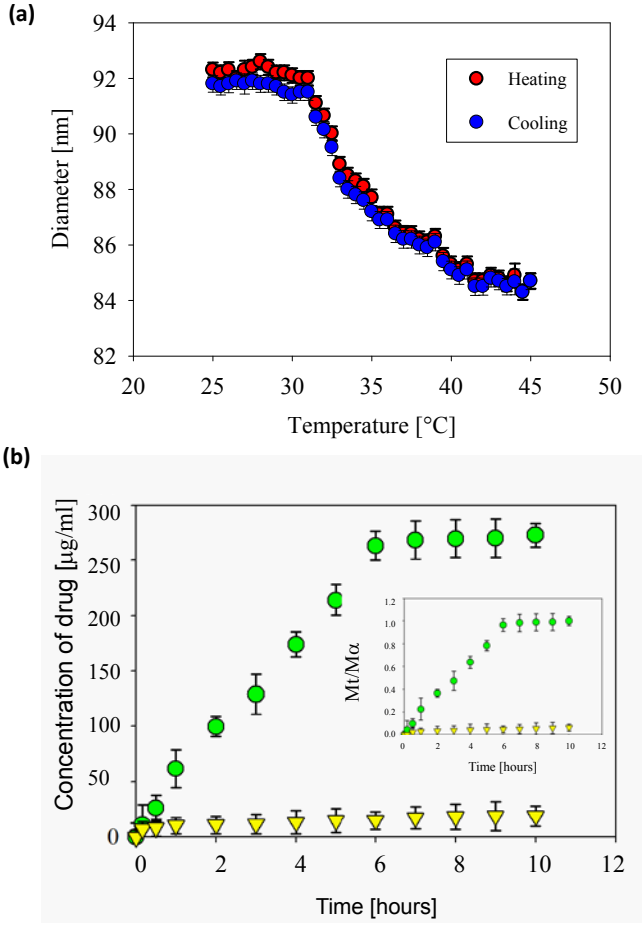

Figure 3: (a) The dependence of average diameter of composite nanoparticles (15% NIPAAm) on temperature. The error bars show standard deviations of particles made in three different batches. The transition temperature is around 32°C. There size transition is nearly reversible. (b) Drug release versus time curve indicating release at room temperature (yellow triangles) and at 40°C (green circles). There is no release at 25°C which is below the transition temperature of the composite particle. The cumulative fractional release is shown as an inset where the maximum amount of drug release value is taken at 40°C for 10 hours; diffusion model parameters have been calculated from these data.

and it requires complicated formulations with Cremophor EL (CrEL), DMSO, or EtOH before parenteral administration [37]. This is undesirable as CrEL is known to induce hypersensitivity reactions and anaphylaxis, and requires patient pretreatment with antihistamines and steroids before administration [38]. A safer administration of 17-AAG can be made by a surfactant free delivery system rather than using harmful surfactants to solubilize the drug. . Therefore, it requires a viable drug carrier for its time-controlled release. The release study of 17-AAG from the nanoparticles was first performed in deionized water. The composite nanoparticles encapsulated with 17-AAG to be tested were divided into two parts. The first portion was kept at room temperature and the second was in a temperature-controlled water bath at 40°C during the duration of the experiment. At regular time intervals, the samples were taken out and then centrifuged at 10,000 rpm for 3 min in a Beckman Coulter tabletop centrifuge and 100 µL of the supernatant was drawn out from release system for analysis. We have also performed DLS experiments on the supernatant to verify the absence of nanoparticles (data not shown; readings of 0 nm).

Cumulative drug release measurements were performed. Figure 3(b) depicts the actual release at 25°C and 40°C and cumulative fractional release (40°C) kinetics of 17-AAG from the drug-loaded nanoparticles. No significant release of the drug was observed at room temperature (25°C). However, at a higher temperature of 40°C, the drug release from the nanoparticles reached a maximum after 7 h. The cumulative fractional drug release (inset of Figure 3(b)) is calculated as M_t/M_∞, where t is the release time, M_t is the amount of drug released at a time t and M_∞ is the amount of drug released at time infinity. Infinity is taken to be when the maximum amount of drug gets released and there is no subsequent release after infinity. The concentration of the drug in the sample solution was read from the calibration curve as the concentration corresponding to the absorbance of the solution. To determine the release mechanisms of the composite nanoparticle system an equation proposed by Yasuda et al. [39] was used, which analyses the release behavior of a solute from a polymer matrix, $M(t) = kt^n$ where M (t) is the amount of drug M (∞) released at time t, $M(\infty)$ is the total amount of drug released at a time ∞ which is taken to be the saturation time when no further amount of drug is released, k is a constant related to the physical properties of the system, and the index, n, is the diffusional component that depends on the release mechanism. When $n<0.5$, the solute is released by Fickian diffusion; when $0.5<n<1.0$, the solute is released by non-Fickian diffusion and when $n=1$, there is zero order release [39]. The calculated n value is 0.73 which indicates the non-Fickian diffusion. The mathematical model indicates that the drug diffusion behavior is non-Fickian and the rate of drug release is due to the combined effect of drug diffusion and polymer response due to increase in temperature.

It was hypothesized that polystyrene/PNIPAAm-silica core-shell nanoparticles are sufficiently small to be taken up by cancer cells. Cell uptake experiments were performed using human prostate cancer cells (50,000/well in 24 well plates). The uptake of the composite nanoparticles by PC3 and PC3-PSMA cells following incubation for 0.5, 1, 1.5 (Supplementary Figure 1) and 5 h (Figure 4) was visualized using confocal microscopy. In Figure 4, at a nanoparticle dosage of 0 (control), 0.025 and 0.05 µg/ml, the human prostate cancer cells take up dye-loaded composite nanoparticles and traffic them throughout the cytoplasm while remaining viable after incubation for 5 h. Visible green fluorescence in Figure 4 suggests that composite nanoparticles are internalized in both the PC3 and PC3-PSMA cells. Initial internalization of nanoparticles in both PC3 and PC3-PSMA cells was observed after 1 h of incubation (Supplementary figure). A control was kept under observation at the different times with no nanoparticles. Uptake was observed at lower concentration of 0.025 µg/ml and at a higher concentration of 0.05 µg/ml. The higher concentration case shows presence of some debris which may be due to some cell death as indicated by cytotoxicity experiments. Nanoparticles could be transported into the cell by either specific (receptor-targeted) or nonspecific cellular uptake mechanisms depending on the surface properties. Since the nanoparticles are not conjugated with any

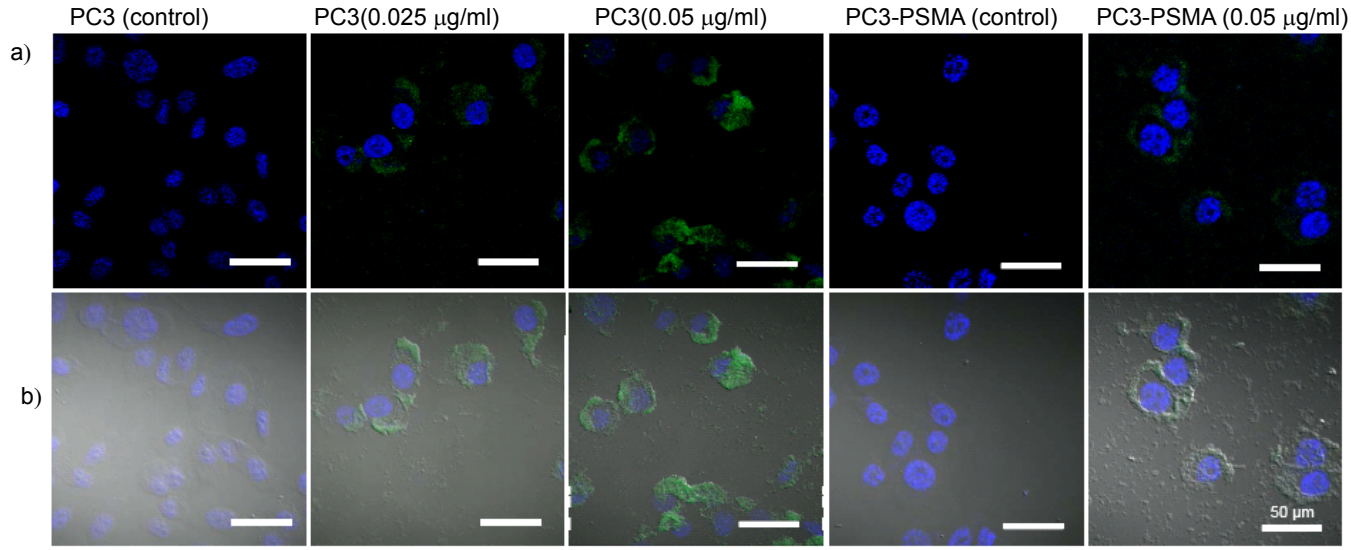

Figure 4: Cellular uptake of BODIPY 493/503 dye -loaded core-shell nanoparticles by PC3 and PC3-PSMA human prostate cancer cell lines following 5 h treatment. Untreated PC3 and PC3-PSMA cells were used as controls. In all cases, cellular nuclei were stained using Hoechst 33258. The top row shows overlays of green (BODIPY) and blue (Hoechst) fluorescence images. The bottom row shows overlays of fluorescence images and their corresponding differential interference contrast (DIC) images.

antibody, the uptake behavior here is nonspecific. Nonspecific uptake of nanoparticles has recently attracted much attention in the development of new strategies for designing efficient nano-carriers, though specific uptake is a more developed strategy as more control is possible and effects on cell functions are easier to predict. Our findings suggest that the thermally sensitive composite nanoparticles can be taken up by prostate cancer cells, which opens new opportunities in controlled drug delivery. Further research in our laboratory will involve conjugation of targeting biomolecules on the surface of these nanoparticles in order to facilitate selective delivery to prostate cancer cells. Eventually, this strategy can result in lower toxicities towards non-malignant cells and other organs *in vivo*.

We next compared the ability of 17-AAG-containing polystyrene/PNIPAAm-silica core-shell nanoparticles (17-AAG-PS/PNIPAAm) to induce death in prostate cancer cells, and compared it with cell death induced by polystyrene-silica nanoparticles (PS), 17-AAG-laoded polystyrene-silica nanoparticles (17-AAG-PS) and polystyrene/PNIPAAm-silica nanoparticles (PS/PNIPAAm). Two-tailed Student's t-test was employed to compare the two groups, 17-AAG-PS/PNIPAAm and PS/PNIPAAm. As seen in Figure 5a, thermoresponsive nanoparticles loaded with 17-AAG (17-AAG-PS/PNIPAAm) induced the greatest dose-dependent death in PC3 cells at nanoparticle dosages from 0.01 to 1 μg/ml compared to other nanoparticle formulations.

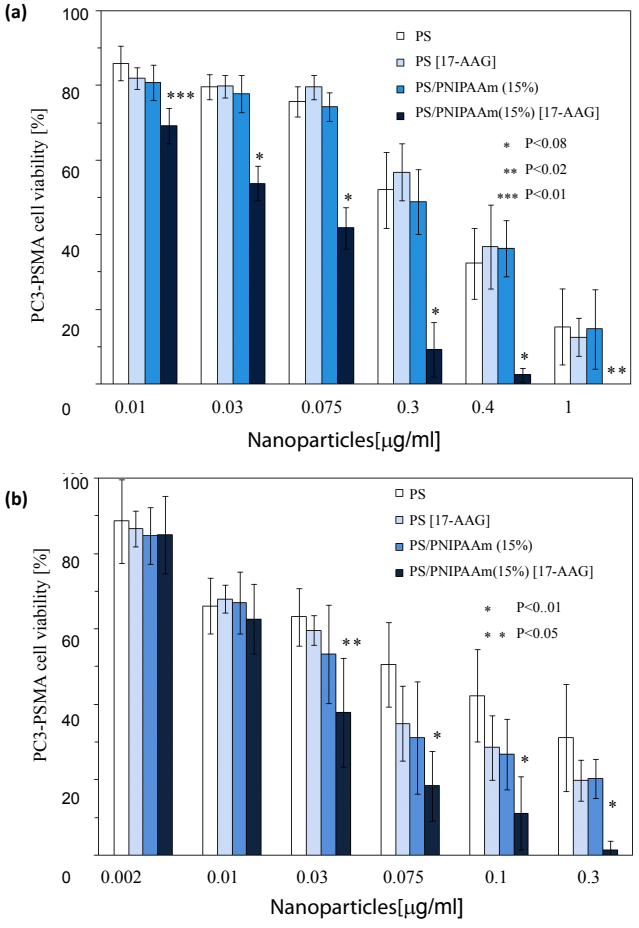

Figure 5: Cytotoxicity of 17-AAG loaded particles against prostate cancer cell lines (a) PC3 (b) PC3-PSMA Two-tailed student's t-test was employed to compare between 17-AAG-PS/PNIPAAm and PS/PNIPAAm treatment.

Drug-loaded nanoparticles are minimally toxic at lower doses (0.01 μg/ml), but induce death in 35 – 90% of the PC3 population at doses from 0.03-0.3 μg/ml. This is statistically significant from other nanoparticle formulations tested under similar conditions (Figure 5a), indicating that uptake and drug release of the 17-AAG containing nanoparticles resulted in death of PC3 cells. The nanoparticles were not as efficacious in inducing death in PC3-PSMA cells compared to PC3 cells (Figure 5b). While 17-AAG containing nanoparticles demonstrated higher average losses in cell viability in PC3-PSMA cells compared to other nanoparticle formulations, these differences were not statistically significant except at the highest concentration (0.3 μg/ml). This can be explained in part by the susceptibility of this cell line to nanoparticles without the drug; while 'bare' nanoparticles do not result in loss of viability of PC3 cells, they induce death in a large population of PC3-PSMA cells in a dose-dependent fashion. In addition, previous results in our laboratory have demonstrated differential therapeutic efficacy in these cell lines due to differential intracellular trafficking and localization of nanoparticles [40,41]. These differences in closely related cell lines underscore the role of the cancer cell phenotype in determining efficacy of delivered nanoparticle therapeutics and are currently under investigation in our laboratories. In addition, it is hypothesized that conjugation of prostate cancer cell specific biomolecules (e.g. antibodies to the Prostate-Specific Membrane Antigen [42]) will help receptor-mediated uptake of these nanoparticles leading to increased efficacies.

Conclusions

The focus of this work was to employ a unique drug delivery vehicle which can be taken up by cancer cells and can release the loaded drug. Polystyrene/PNIPAAm-silica core-shell nanoparticles were successfully synthesized with N-isopropylacrylamide incorporated into the core of the nanocomposite as a co-monomer. The work has demonstrated the temperature sensitivity, controlled drug release properties of the synthesized core-shell nanoparticles, and their effectiveness for inducing death of human prostate cancer cells. The collapse of the PNIPAAm resulted in the shrinkage of composite particles at temperatures above the LCST which makes them promising as a unique drug delivery vehicle. Future work will focus on further understanding the delivery mechanism, investigation of targeted nanoparticles, and modification of the transition temperature of the composite particles to just above physiological temperature (i.e. 37°C) for *in vivo* drug delivery for destruction of the human prostate cancer tumors.

Acknowledgements

We acknowledge Professor.Paul Westerhoff and the Center for Solid State Sciences at Arizona State University for instrument usage. We gratefully thank Professor Deirdre Meldrum, Director of the Center for Biosignatures Discovery Automation (CBDA) at the Biodesign Institute, Arizona State University for access to the Nikon confocal microscope used in the current study. We also thank Matt Christensen, a graduate student in Dr. Rege's laboratory and Dr. Honor Glenn from CBDA for excellent technical assistance with confocal microscopy. This work is financially supported by the National Science Foundation through grant CBET-0918282 to LD and grant CBET-0829128 to KR.

References

1. Jain PK, Lee KS, El-Sayed IH, El-Sayed MA (2006) Calculated Absorption and Scattering Properties of Gold Nanoparticles of Different Size, Shape, and Composition: Applications in Biological Imaging and Biomedicine. J Phys Chem 110: 7238-7248.

2. Liu C, Zhang ZJ (2001) Size-Dependent Superparamagnetic Properties of Mn Spinel Ferrite Nanoparticles Synthesized from Reverse Micelles. Chemical Materials 13: 2092-2096.

3. Ding BS, Dziubla T, Shuvaev VV, Muro S, Muzykantov VR (2006) Advanced

drug delivery systems that target the vascular endothelium. Molecular Interventions 6: 98-112.

4. Sanchez C, Julian B, Belleville P, Popall M (2005) General Strategies for the Design of Functional Hybrid Materials. J Mater Chem 15: 35-36.
5. Caruso F (2000) Hollow Capsule Processing through Colloidal Templating and Self-Assembly. Chem Eur 6: 413-419.
6. Huang HY, Remsen EE, Kowalewski T, Wooley KL (1999) Nanocages Derived from Shell Cross-Linked Micelle Templates. J Am Chem Soc 121: 3805-3806.
7. Lynch DE, Nawaz Y, Bostrom T (2005) Preparation of Sub-micrometer Silica Shells Using Poly(1-methylpyrrol-2-ylsquaraine) Langmuir 21: 6572-6575
8. Ding XF, Jiang YQ, Yu KF, Hari-Bala, Tao NN, et al. (2004) Silicon dioxide as coating on polystyrene nanoparticles in situ emulsion polymerization Mater Lett 58: 1722-1725.
9. Dokoutchaev A, James JT, Koene SC, Pathak S, Prakash GKS, et al. (1999) Colloidal Metal Deposition onto Functionalized Polystyrene Microspheres. Chem Mater 11: 2389-2399.
10. Caruso F (2001) Nanoengineering of Particle Surfaces. Adv Mater 13: 11-22.
11. Caruso F, Susha AS, Giersig M, Möhwald H (1999) Magnetic Core–Shell Particles: Preparation of Magnetite Multilayers on Polymer Latex Microspheres. Adv Mater 11: 950-953.
12. Caruso RA, Susha A, Caruso F (2001) Multilayered Titania, Silica, and Laponite Nanoparticle Coatings on Polystyrene Colloidal Templates and Resulting Inorganic Hollow Spheres. Chem Mater 13: 400-409.
13. Bon SAF, Colver PJ (2007) Pickering Stabilization as a Tool in the Fabrication of Complex Nanopatterned Silica Microcapsules. Langmuir 23: 9527-9530.
14. Cauvin S, Colver PJ, Bon SAF (2005) Pickering Stabilized Miniemulsion Polymerization: Preparation of Clay Armored Latexes. Macromolecules 38: 7887-7889.
15. Schmid A, Fujii S, Armes SP, Leite CAP, Galembeck F, et al. (2007) Polystyrene-Silica Colloidal Nanocomposite Particles Prepared by Alcoholic Dispersion Polymerization. Chemistry of Materials 19: 2435-2445.
16. Yang J, Hasell T, Wang WX, Li J, Brown PD, et al. (2008) Preparation of Hybrid Polymer Nanocomposite Microparticles by a Nanoparticle Stabilised Dispersion Polymerisation. J Mater Chem 18: 998-1001.
17. Duan LL, Chen M, Zhou S, Wu L (2009) Synthesis and Characterization of Poly (N-isopropylacrylamide) / Silica Composite Colloidsomes via Inverse Pickering Emulsion Polymerization. Langmuir 25: 3467-3472.
18. Gao Q, Wang C, Liu H, Wang C, Liu X, et al. (2009) Suspension polymerization based on inverse Pickering emulsion droplets for thermo-sensitive hybrid microcapsules with tunable supracolloidal structures. Polymer 50: 2587-2594
19. Voorn DJ, Ming W, van Herk AM (2006) Encapsulation of Platelets by Physical and Chemical Approaches. Macromol Symp 245: 584-590.
20. Bourgeat-Lami E, Lang J (1998) Encapsulation of Inorganic Particles by Dispersion Polymerization in Polar Media: 1. Silica Nanoparticles Encapsulated by Polystyrene. J Colloid Interface Sci 197: 293-308.
21. Gu S, Kondo T, Konno M (2004) Preparation of silica–polystyrene core–shell particles up to micron sizes. J Colloid Interface Sci 272: 314-320.
22. Guo YK, Wang MY, Zhang HQ, Liu GD, Zhang LQ, et al. (2008) The surface modification of nanosilica, preparation of nanosilica/acrylic core-shell composite latex, and its application in toughening PVC matrix. J Appl Polym Sci 107: 2671-2680.
23. Nagao D, Yokoyama M, Saeki S, Kobayashi Y, Konno M (2008) Preparation of composite particles with magnetic silica core and fluorescent polymer shell. Colloid Polym Sci 286:959-964.
24. Tianbin W, Yangchuan K (2006) Preparation of silica-PS composite particles and their applications in PET. Eur Polym J 42: 274-285.
25. Barthet C, Hickey AJ, Cairns DB, Armes SP (1999) Synthesis of Novel Polymer Silica Colloidal Nanocomposites via Free-Radical Polymerization of Vinyl Monomers. Adv Mater 11:408-410.
26. Lee J, Hong CK, Choe S, Shim SE (2007) Synthesis of polystyrene/ silica composite particles by soap-free emulsion polymerization using positively charged colloidalsilica. J Colloid Interface Sci 310: 112-120.
27. Schild HG (1992) Poly(N-isopropylacrylamide): experiment, theory and application. Progress in Polymer Science 17: 163-249.
28. Teo BM, Prescott SW, Price GJ, Grieser F, Ashokkumar M (2010) Synthesis of temperature responsive poly(N-isopropylacrylamide) using ultrasound irradiation. J Phy Chem B 114: 3178-3184.
29. Qiu Y, Park K (2001) Environmentally-sensitive polymer hydrogels, in Triggered Release in Drug Delivery Systems. Adv Drug Deliv Rev 53: 321-339.
30. Wang H, An Y, Huang N, Ma R, Li J, et al. (2008) Contractive Polymeric Complex Micelles as Thermo-Sensitive Nanopumps. Macromol Rapid Commun 29: 1410-1414.
31. Wei H, Zhang X, Chen W, Cheng S, Zhuo R (2007) Self-assembled thermosensitive micelles based on poly(L-lactide-star block-*N*-isopropylacrylamide) for drug delivery. J Biomed Mater Res Part A 83: 980-989.
32. Gong MC, Latouche J, Krause A, Heston WDW, Bander NH, et al. (1999) Cancer patient T cells genetically targeted to prostate-specific membrane antigen specifically lyse prostate cancer cells and release cytokines in response to prostate-specific membrane antigen. Neoplasia 1: 123-127.
33. Han, Armes SP (2003) Preparation and characterization of polypyrrole–silica colloidal nanocomposites in water–methanol mixtures. J Colloid Interface Sci 262: 418-427.
34. Ma H, Dai LL (2009) Synthesis of Polystyrene-Silica Composite Particles via One-Step Nanoparticle- Stabilized Emulsion. J. Colloid Interface Sci. 333:807-811.
35. Ma H, Luo MX, Sanyal S, Rege K, Dai LL (2010) The One-Step Pickering Emulsion Polymerization Route for Synthesizing Organic-Inorganic Nanocomposite Particles. Materials 3: 1186-1202.
36. Duracher D, Sauzedde F, Elaissari A, Perrin A, Pichot C (1998) Cationic amino-containing *N* -isopropyl- acrylamide–styrene copolymer latex particles: 1-Particle size and morphology vs. polymerization process. Colloid Polym Sci 276: 219-231.
37. Shin HC, Alani AW, Rao DA, Rockich NC, Kwon GS (2009) Multi-drug loaded polymeric micelles for simultaneous delivery of poorly soluble anticancer drugs. J Control Release140: 294-300.
38. Xiong M, Yáñez J, Kwon G, Davies N, Forrest M (2009) A Cremophor-Free Formulation for Tanespimycin (17-AAG) using PEO-b-PDLLA Micelles: Characterization and Pharmacokinetics in Rats. J Pharm Sci 4: 1577-1586.
39. Yasuda H, Lamaze CE, Ikenberry LD (1968) Permeability of solutes through hydrated polymer membranes. Part I. Diffusion of sodium chloride. Macromol Chem Phys 118: 19-35.
40. Barua S, Rege K (2010) The Influence of Mediators of Intracellular Trafficking on Transgene Expression Efficacy of Polymer-Plasmid DNA Complexes. Biomaterials. 22: 894-902.
41. Barua S, Rege K (2009) Cancer-Cell-Phenotype-Dependent Differential Intracellular Trafficking of Unconjugated Quantum Dots. Small 5: 370-376.
42. Rege K, Patel SJ, Megeed Z, Yarmush ML (2007) Amphipathic peptide-based fusion peptides and immunoconjugates for the targeted ablation of prostate cancer cells. Cancer Res 67: 6368-6375.